

Rheology of an emulsion of viscoelastic drops in steady shear

Nishith Aggarwal, Kausik Sarkar*

Department of Mechanical Engineering, University of Delaware, Newark, DE 19716, United States

Received 7 May 2007; received in revised form 7 September 2007; accepted 24 September 2007

Abstract

Steady shear rheology of a dilute emulsion with viscoelastic inclusions is numerically investigated using direct numerical simulations. Batchelor's formulation for rheology of a viscous emulsion is extended for a viscoelastic system. Viscoelasticity is modeled using the Oldroyd-B constitutive equation. A front-tracking finite difference code is used to numerically determine the drop shape, and solve for the velocity and stress fields. The effective stress of the viscoelastic emulsion has three different components due to interfacial tension, viscosity difference (not considered here) and the drop phase viscoelasticity. The interfacial contributions – first and second normal stress differences and shear stresses – vary with Capillary number in a manner similar to those of a Newtonian system. However the shear viscosity decreases with viscoelasticity at low Capillary numbers, and increases at high Capillary numbers. The first normal stress difference due to interfacial contribution decreases with increasing drop phase viscoelasticity. The first normal stress difference due to the drop phase viscoelasticity is found to have a complex dependence on Capillary and Deborah numbers, in contrast with the linear mixing rule. Drop phase viscoelasticity does not contribute significantly to effective shear viscosity of the emulsion. The total first normal stress difference shows an increase with drop phase viscoelasticity at high Capillary numbers. However at low Capillary numbers, a non-monotonic behavior is observed. The results are explained by examining the stress field and the drop shape. © 2007 Elsevier B.V. All rights reserved.

Keywords: Oldroyd-B; Rheology; Viscoelastic; Emulsion; Drop

1. Introduction

For the synthesis of emulsions with desirable macroscopic properties, it is imperative that we understand the relationship between its 'microstructure' and rheological properties [1]. The earliest attempts to relate the rheology with microstructures are due to Einstein [2,3] and Taylor [4], who determined the effective viscosity for dilute suspensions and emulsions, respectively. Oldroyd [5,6] showed that elastic properties in dilute emulsions with Newtonian components arises as a result of the interfacial tension. Schowalter et al. [7] explicitly demonstrated, by performing a small deformation analysis of a single drop, that in a dilute emulsion of such drops there exist a positive first and a negative second normal stress differences both quadratic in shear rate, i.e. $N_1, N_2 \propto \dot{\gamma}^2$. Choi and Schowalter [8] extended the analysis to a semi-dilute emulsions with Newtonian components.

Batchelor [9] rigorously developed a theory for the stress in a homogeneous emulsion. It predicts that the effective stress in

a Newtonian emulsion contains two elements—the component contribution due to the difference in viscosity between the two phases and the interfacial contribution due to the surface tension at the interface between the two phases. Batchelor expressed the excess stress in terms of an interface tensor [10,11]. Given the dispersed phase morphology, the theory allows computation of both transient and steady rheology of an emulsion.

For droplet type morphologies in a dilute emulsion with Newtonian components, there has been significant effort to describe the evolution of a drop, assuming an ellipsoidal shaped drop described by a second-order phenomenological tensor [12–18]. Using the model of [15] Jansseune et al. [19,20] related the rheology with the droplet orientation angle, which in turn is related to the Capillary number. They proposed a method of measuring droplet size distribution from rheology using such relations and applied it to PIB/PDMS system. The transient emulsion rheology for the same system was also investigated using the droplet model [20].

In a concentrated emulsion, droplets can undergo large deformation, breakup (for Capillary number $Ca > Ca_{crit}$) and coalescence, and the final morphology becomes quite complicated. To investigate such a complex emulsion, Doi and Ohta [21] proposed a simple phenomenological model for the

* Corresponding author. Tel.: +1 302 831 0149.

E-mail addresses: sarkar@udel.edu, sarkar@me.udel.edu (K. Sarkar).

evolution of the Batchelor's interface tensor, and predicted a linear scaling for both shear ($\sigma_{12} \propto \dot{\gamma}$) and the first normal stresses ($N_1 \propto |\dot{\gamma}|$) (in contrast to $N_1 \propto \dot{\gamma}^2$ more commonly observed and predicted by other theories such as [8]). The reason for the anomalous scaling is that the droplet size instead of being fixed as in other theories, is determined dynamically as $\propto 1/\dot{\gamma}$, by the breakup and coalescence. Doi–Ohta scalings have been observed experimentally for a variety of systems [22–24] including systems with viscoelastic components, when excess stress contribution from the interface is isolated by using a linear mixing rule for the viscoelastic component contributions [22,25]. Other similar interface theories [26–29] with component to incorporate length scales of individual droplets in the theory [30–32] have been developed.

Blends with non-Newtonian components, however, have not been studied in much detail. Palierne [33,34] studied emulsions of linearly viscoelastic components and developed a model for the bulk modulus at arbitrary concentrations of spherical inclusions with interfacial tension. The model successfully described rheological behavior of molten polymers in oscillatory flows at high and low frequencies [24,35,36]. Bousmina [37] reworked Kerner's [38] model by including the effect of interfacial tension as an additive modulus (=surface tension/radius) to the total elastic modulus of the inclusion, to describe rheology of linearly viscoelastic emulsions. Recently, Yu et al. [39] developed a small drop deformation theory for viscoelastic systems and extended Batchelor's formulation to describe the rheology of blends with linearly viscoelastic components.

It should also be noted that for the experimental studies mentioned above, the viscoelastic component contributions were neglected [19,23,24], or estimated using linear mixing rule [20,22,25,40]. It therefore becomes important to investigate the validity of such assumption with detailed measurement or computation of component contributions.

In this paper we investigate the steady shear rheological behavior of an emulsion of non-Newtonian inclusions in a Newtonian matrix, using an extension of Batchelor's stress formulation [9]. We explicitly compute the component and the interface contributions from the simulated drop shape and viscous and viscoelastic stress fields. We restrict ourselves to the dilute case where the droplet interactions can be neglected so that we can use a single drop simulation to compute the emulsion rheology. We have recently completed such an investigation of an Oldroyd-B drop deforming in a Newtonian matrix in steady shear [42] using the front-tracking method [41–43]. For other recent viscoelastic drop deformation studies we refer the interested reader to [42,44–48] and to the references in Aggarwal and Sarkar [42].

The ability of the front-tracking method to accurately describe a moving interface is critical for determining the interfacial rheological response. Furthermore, the explicit computation of the viscous and the viscoelastic stress field allows direct evaluation of the component contributions for the first time. We should mention that the numerical method can be extended to concentrated emulsions albeit at a significantly larger computational cost. Recently, a similar computational technique was used to investigate the non-Newtonian rheology of a dilute emul-

sion with viscous components in an oscillating extensional flow [49–51] and a steady shear flow with finite inertia [52]. Note that for purely viscous emulsions, numerical computations have been performed using boundary element method by a number of groups [40,53,54]. However, for viscoelastic emulsions such computation has not been previously undertaken.

2. Problem formulation

2.1. Governing equations

The single drop problem is described in detail by Aggarwal and Sarkar [42]. The incompressible flow is governed by the momentum and mass conservation equations in the entire domain Ω , consisting of the matrix (continuous) phase Ω_c and the drop (dispersed) phase Ω_d (Fig. 1):

$$\frac{\partial(\rho\mathbf{u})}{\partial t} + \nabla \cdot (\rho\mathbf{u}\mathbf{u}) = - \int_{\partial\mathbf{B}} d\mathbf{x}_{\mathbf{B}} \kappa \mathbf{n} \Gamma \delta(\mathbf{x} - \mathbf{x}_{\mathbf{B}}) + \nabla \cdot \boldsymbol{\tau}, \quad (1)$$

$$\nabla \cdot \mathbf{u} = 0. \quad (2)$$

Here, Γ is the interfacial tension (constant), $\partial\mathbf{B}$ represents the drop surface consisting of points $\mathbf{x}_{\mathbf{B}}$, κ is the local curvature, \mathbf{n} is the outward normal, $\delta(\mathbf{x} - \mathbf{x}_{\mathbf{B}})$ is the three-dimensional Dirac-Delta function and $\boldsymbol{\tau}$ is the total stress given by

$$\boldsymbol{\tau} = -p\mathbf{I} + \mathbf{T} + \boldsymbol{\mu}_s\mathbf{D}, \quad (3)$$

where p is the pressure, \mathbf{T} is the extra stress (viscoelastic stress) due to presence of the polymer, $\boldsymbol{\mu}_s$ is the solvent viscosity and $\mathbf{D} = (\nabla\mathbf{u}) + (\nabla\mathbf{u})^T$ is the strain rate tensor. For the viscoelastic drop phase, we use the Oldroyd-B constitutive equation for the extra stress tensor, having a single relaxation time λ :

$$\lambda \left\{ \frac{\partial\mathbf{T}}{\partial t} + \mathbf{u} \cdot \nabla\mathbf{T} - (\nabla\mathbf{u})\mathbf{T} - \mathbf{T}(\nabla\mathbf{u})^T \right\} + \mathbf{T} = \mu_p\mathbf{D}, \quad (4)$$

μ_p is the polymeric viscosity in the Oldroyd-B phase. For $\lambda = 0$, we obtain the Newtonian fluid in the matrix phase. The Oldroyd-B fluid shows a constant shear viscosity $\mu = \mu_s + \mu_p$, where μ_s is the solvent viscosity. Shear flow of an Oldroyd-B fluid gives rise to a first normal stress difference, N_1 proportional to the square of the shear rate ($\dot{\gamma}$). Non-Newtonian rheology arises because of an anisotropic contribution from the deformed drop

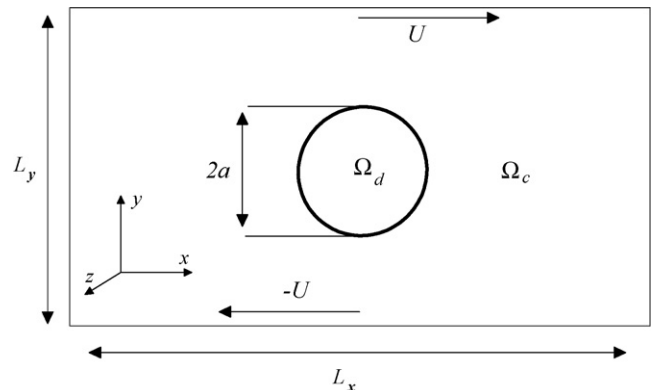


Fig. 1. Schematic of the domain of computation.

shape as well as the presence of viscoelastic stresses in the drop phase. We note that the single equation (Eq. (1)) in the whole domain is mathematically equivalent to the usual two-equation formulation with continuity in the shear stress and jump in the normal stress due to surface tension (represented by the delta function term).

We use the initial drop radius a as a length scale and inverse strain rate $\dot{\gamma}^{-1}$ as a time scale to define the non-dimensional parameters: Reynolds number $Re = \rho_m a^2 \dot{\gamma} / \mu_m$; Capillary number $Ca = (\mu_m a \dot{\gamma}) / \Gamma$; Deborah number $De = \lambda \dot{\gamma}$; density ratio $\lambda_\rho = \rho_d / \rho_m$ (ρ_d is the drop phase density and ρ_m is the matrix phase density); viscosity ratio $\lambda_\mu = \mu_d / \mu_m$ (μ_d is the total drop viscosity and μ_m is matrix viscosity). We define, for the Oldroyd-B drop, $\beta = \mu_{pd} / \mu_d = \mu_{pd} / (\mu_{sd} + \mu_{pd})$, where μ_{sd} is the drop solvent viscosity and μ_{pd} is the drop polymeric viscosity. Here we study only the density and viscosity matched system (i.e. $\lambda_\mu = \lambda_\rho = 1$). Also, we study low but finite inertia case with $Re = 0.1$, because the explicit nature of the code precludes computation of solutions in the exact Stokes limit. $\beta = 0.5$ for all our computations except when mentioned otherwise.

2.2. Bulk stress in an emulsion with viscoelastic inclusions

Following Batchelor [9], the average stress in an emulsion can be expressed as a volume average:

$$\begin{aligned} \sigma^{ave} &= \frac{1}{V} \int_V \sigma \, dV = \frac{1}{V} \int_{V-\Sigma V_0} \sigma \, dV \\ &+ \frac{1}{V} \sum \int_{V_0} \sigma \, dV - \frac{\Gamma}{V} \sum \int_{A_0} \left(\mathbf{nn} - \frac{\mathbf{I}}{3} \right) \, dA, \end{aligned} \quad (5)$$

where V is a representative volume of the emulsion, consisting of identical droplets of volume V_0 and interfacial area A_0 . The summation is therefore over individual drops. The last term in the equation above represents contributions due to the surface tension at the phase boundaries. For a Newtonian suspending fluid in the volume $V - \Sigma V_0$, the average stress can be re-expressed as

$$\begin{aligned} \sigma^{ave} &= \frac{1}{V} \int_{V-\Sigma V_0} [-p\mathbf{I} + \mu_m(\nabla\mathbf{u} + \nabla\mathbf{u}^T)] \, dV \\ &+ \frac{1}{V} \sum \int_{V_0} \sigma \, dV - \frac{\Gamma}{V} \sum \int_{A_0} \left(\mathbf{nn} - \frac{\mathbf{I}}{3} \right) \, dA. \end{aligned} \quad (6)$$

Defining, the bulk gradient tensor in the representative volume:

$$\nabla\mathbf{U} + \nabla\mathbf{U}^T = \frac{1}{V} \int_V (\nabla\mathbf{u} + \nabla\mathbf{u}^T) \, dV \quad (7)$$

we can re-express the average stress:

$$\begin{aligned} \sigma^{ave} &= \frac{1}{V} \int_{V-\Sigma V_0} [-p\mathbf{I} + \mu_m(\nabla\mathbf{U} + \nabla\mathbf{U}^T)] \, dV \\ &+ \frac{1}{V} \sum \int_{V_0} \sigma \, dV - \frac{\mu_m}{V} \sum \int_{A_0} (\mathbf{un} + \mathbf{nu}) \, dA \\ &- \frac{\Gamma}{V} \sum \int_{A_0} \left(\mathbf{nn} - \frac{\mathbf{I}}{3} \right) \, dA. \end{aligned} \quad (8)$$

For each of the viscoelastic inclusions with both Newtonian (due to the solvent viscosity) and extra stress \mathbf{T} (due to the polymer) contributions:

$$\begin{aligned} \frac{1}{V} \int_{V_0} \sigma \, dV &= \frac{1}{V} \int_{V_0} \left[-p\mathbf{I} + \frac{\mu_{sd}}{V} (\nabla\mathbf{u} + \nabla\mathbf{u}^T) + \mathbf{T} \right] \, dV \\ &= \frac{1}{V} \int_{V_0} -p\mathbf{I} \, dV + \frac{\mu_d}{V} \int_{V_0} (\mathbf{un} + \mathbf{nu}) \, dA \\ &+ \frac{1}{V} \int_{V_0} (\mathbf{T} - \mu_{pd}\mathbf{D}) \, dV, \end{aligned} \quad (9)$$

where μ_{sd} is the solvent viscosity of the dispersed phase. Note that the effective viscous part of the polymeric part in \mathbf{T} is subtracted to separate the pure viscoelastic part. For an emulsion with viscoelastic dispersions:

$$\begin{aligned} \sigma^{ave} &= \frac{1}{V} \int_V [-p\mathbf{I} + \mu_m(\nabla\mathbf{U} + \nabla\mathbf{U}^T)] \, dV \\ &+ \frac{1}{V} \sum \int_{V_0} (\mathbf{T} - \mu_{pd}\mathbf{D}) \, dV \\ &+ \frac{\mu_d - \mu_m}{V} \sum \int_{A_0} (\mathbf{un} + \mathbf{nu}) \, dA \\ &- \frac{\Gamma}{V} \sum \int_{A_0} \left(\mathbf{nn} - \frac{\mathbf{I}}{3} \right) \, dA, \end{aligned} \quad (10)$$

or,

$$\sigma^{ave} = -p^{ave}\mathbf{I} + \boldsymbol{\tau}^{ave} + \sigma^{excess}, \quad (11)$$

p^{ave} represents an isotropic contribution, $\boldsymbol{\tau}^{ave} = \mu_m(\nabla\mathbf{U} + \nabla\mathbf{U}^T)$ represents the deviatoric stress in the emulsion in absence of the dispersed phase. σ^{excess} represents the excess stress due to the presence of the dispersed phase. It has the following separately identifiable components:

$$\sigma^{excess} = \sigma^{el} + \sigma^{vis} + \sigma^{int}, \quad (12)$$

where

$$\sigma^{el} = \frac{1}{V} \sum \int_{V_0} (\mathbf{T} - \mu_{pd}\mathbf{D}) \, dV, \quad (13)$$

$$\sigma^{vis} = \frac{\mu_d - \mu_m}{V} \sum \int_{A_0} (\mathbf{un} + \mathbf{nu}) \, dA, \quad (14)$$

and,

$$\sigma^{int} = -\Gamma\mathbf{q}, \quad \mathbf{q} = \frac{1}{V} \sum \int_{A_0} \left(\mathbf{nn} - \frac{\mathbf{I}}{3} \right) \, dA, \quad (15)$$

σ^{el} and σ^{vis} are the component contributions, the former is a contribution due to the viscoelasticity of the drop phase and the latter the component stress arising due to a difference in the viscosities of the phases. σ^{int} is the interfacial contribution to the excess stress. For a viscosity matched system $\sigma^{vis} = 0$. In the limit of the relaxation time of the drop phase $\lambda \rightarrow 0$, we expect no viscoelastic component contribution to the excess stress. Note that σ^{el} has been defined in Eq. (13) to achieve the correct Newtonian limit.

In a dilute emulsion, droplets do not interact. Stress contribution of each inclusion is independent and therefore can be expressed in terms of the volume fraction $\Phi = mV_0/V$. Thus,

$$\begin{aligned} \boldsymbol{\sigma}^{\text{int}} &= -\Gamma \mathbf{q}, & \mathbf{q} &= \phi \mathbf{q}_d, & \mathbf{q}_d &= \frac{1}{V_0} \int_{A_0} (\mathbf{nn} - \frac{\mathbf{I}}{3}) dA, \\ \boldsymbol{\sigma}^{\text{el}} &= \phi \frac{1}{V_0} \int_{V_0} (\mathbf{T} - \mu_{\text{pd}} \mathbf{D}) dV. \end{aligned} \quad (16)$$

The non-dimensional stress components are

$$\begin{aligned} \Sigma^{\text{int}} &= \frac{\boldsymbol{\sigma}^{\text{int}}}{\mu_m \dot{\gamma}} = \phi \Sigma_d^{\text{int}}, & \Sigma_d^{\text{int}} &= -\frac{\Gamma}{\mu_m \dot{\gamma}} \\ \mathbf{q}_d &= -\frac{a}{Ca} \mathbf{q}_d, \end{aligned} \quad (17)$$

$$\begin{aligned} \Sigma^{\text{el}} &= \frac{\boldsymbol{\sigma}^{\text{el}}}{\mu_m \dot{\gamma}} = \phi \Sigma_d^{\text{el}}, \\ \Sigma_d^{\text{el}} &= \frac{1}{\mu_m \dot{\gamma} V_0} \int_{V_0} (\mathbf{T} - \mu_{\text{pd}} \mathbf{D}) dV. \end{aligned} \quad (18)$$

The non-dimensional excess stresses are given by

$$\Sigma^{\text{excess}} = \phi \Sigma_d^{\text{excess}} = \Sigma^{\text{int}} + \Sigma^{\text{el}} = \phi \left(\Sigma_d^{\text{int}} + \Sigma_d^{\text{el}} \right). \quad (19)$$

The constitutive properties of this system in shear flow is entirely determined by the effective viscosity μ_e , first normal stress difference N_1 and second normal stress difference N_2 . According to above definitions (subscript d has been dropped from above) and from Eq. (11):

$$\frac{\mu_e}{\mu_m} = 1 + \Sigma_{12}^{\text{int}} + \Sigma_{12}^{\text{el}}, \quad (20)$$

$$N_1 = N_1^{\text{int}} + N_1^{\text{el}} = (\Sigma_{11}^{\text{int}} - \Sigma_{22}^{\text{int}}) + (\Sigma_{11}^{\text{el}} - \Sigma_{22}^{\text{el}}), \quad (21)$$

$$N_2 = N_2^{\text{int}} + N_2^{\text{el}} = (\Sigma_{22}^{\text{int}} - \Sigma_{33}^{\text{int}}) + (\Sigma_{22}^{\text{el}} - \Sigma_{33}^{\text{el}}). \quad (22)$$

2.3. Numerical method

We simulate the single-drop-in-a-shear problem using a front-tracking finite difference method. The method is described in detail in Aggarwal and Sarkar [42]. Here we provide a brief sketch. We consider a computational domain containing a Newtonian matrix with an initially spherical Oldroyd-B drop (of initial radius a) suspended at its centre. The matrix fluid is subjected to a simple shear flow with shear rate $\dot{\gamma}$. The front-tracking method treats the entire system as a single phase, with material properties (density, viscosity and relaxation time) varying sharply in a thin region of width $4\Delta x$ (Δx is the grid spacing) across the interface. The surface tension is represented as a distributed force over this diffused region by choosing a smooth representation for the Dirac-Delta function as shown in Eq. (1). A three-dimensional staggered grid is used for the entire domain on which the momentum and the Oldroyd-B equations are solved. The velocity and stress fields are solved for by an operator-splitting/projection finite-difference method. We

have developed a new algorithm for viscoelastic constitutive equation [42,43]. A triangular mesh is used to discretize the drop surface. This triangular grid is adaptively refined to avoid excessive mesh distortion. The velocity from the regular grid is interpolated to the triangular grid for front advection. We use an explicit method, which suffers from severe restrictions at low Reynolds numbers. To overcome these difficulties we use an ADI method.

The triangular mesh at the drop surface enables us to compute the excess interfacial stress using Eq. (15). In our formulation, the viscoelastic contribution to the excess stress is in the form of a volume integral of viscoelastic stress \mathbf{T} [Eq. (18)]. We simply use node values in each cell multiplied by the cell volume to compute the integral as a Riemann sum. Note that we calculate and plot only the single drop contributions (19) to the excess stress. Convergence in these stress values with grid refinement has been thoroughly checked. We present our results in the next section.

3. Results

We have used an initial drop radius α , box size of $L_x/a = 10$, $L_y/a = 10$ and $L_z/a = 5$ (Fig. 1) and a grid resolution of $96 \times 96 \times 48$ for our steady shear computations. Convergence and box size independence have been carefully established for the rheological contributions calculated in this study. In Fig. 2, we show convergence of the individual stress components with grid refinement for parameter values $Ca = 0.3$ and $De = 2$. The error in each stress component is measured relative to and scaled with the value Σ^{128} at $128 \times 128 \times 64$ resolution; N is the number of grid points along the x -direction. The interfacial stresses show N^2 convergence. Furthermore, in view of the dilute emulsion results (19), we present our results in terms of the contribution from the single drop. Note that all the single

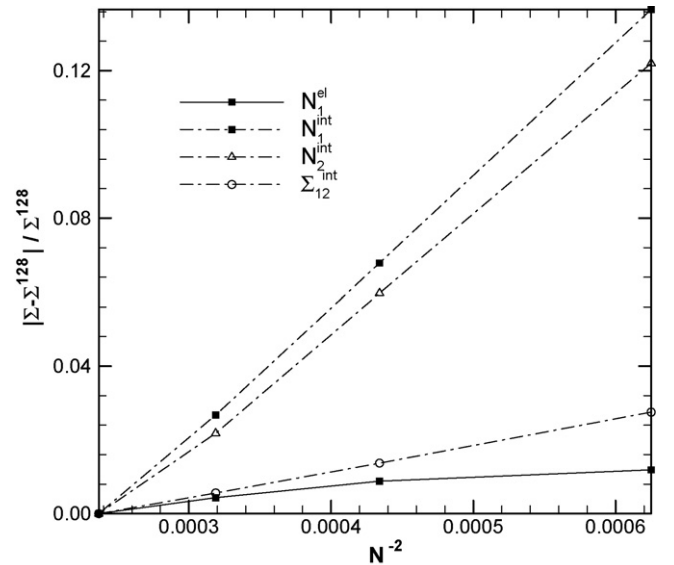


Fig. 2. Convergence of stresses. N is the number of grid points in the x - and y -direction.

drop excess stress components presented here have been normalized with $\mu_m \dot{\gamma}$ as per Eqs. (17) and (18). As we mentioned before, we drop the subscript d representative of the single drop nature of these terms.

3.1. Interfacial stresses

First, we examine the interfacial contributions to the effective stress in the emulsion. Note that the interfacial part is completely determined by the drop shape. Assuming an ellipsoidal drop shape, the interfacial stress contributions have the following correlation with the drop morphology [19]:

$$N_1^{int} = -\frac{a}{Ca V_0} \int_{A_0} (n_{1'}^2 - n_{2'}^2) \cos 2\theta \, dA, \quad (23)$$

$$\Sigma_{12}^{int} = -\frac{a}{Ca V_0} \int_{A_0} (n_{1'}^2 - n_{2'}^2) \frac{\sin 2\theta}{2} \, dA. \quad (24)$$

Therefore,

$$\frac{N_1^{int}}{\Sigma_{12}^{int}} = 2 \cot(2\theta), \quad (25)$$

where θ is the orientation of the drop with the flow direction, $(n_{1'}, n_{2'})$ are components of normal \mathbf{n} to the interface, in a Cartesian coordinate system coinciding with the major and minor axes of the ellipsoid.

In Fig. 3a, we plot the interfacial contributions to the shear viscosity as a function of the Capillary number. An emulsion with purely viscous components shows shear thinning at high shear rates. Our numerical simulation for $De=0$ predicts the same, i.e. the shear viscosity decreases with Capillary number.

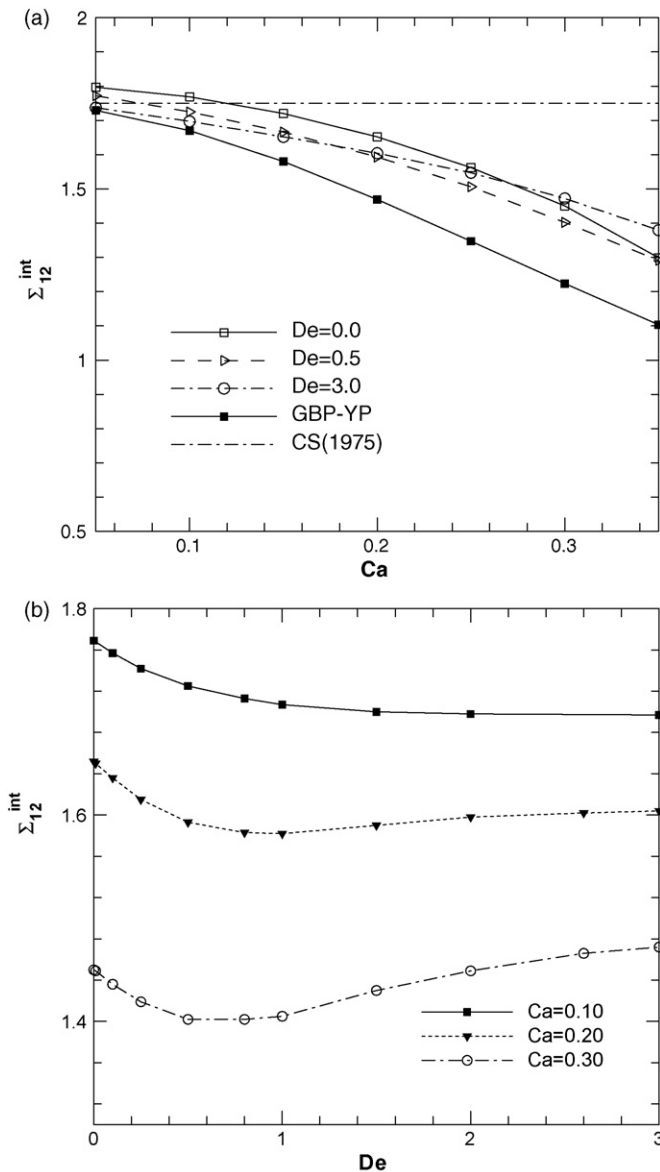


Fig. 3. (a) Interfacial shear stress variations with Ca . (b) Interfacial shear stress variations with De .

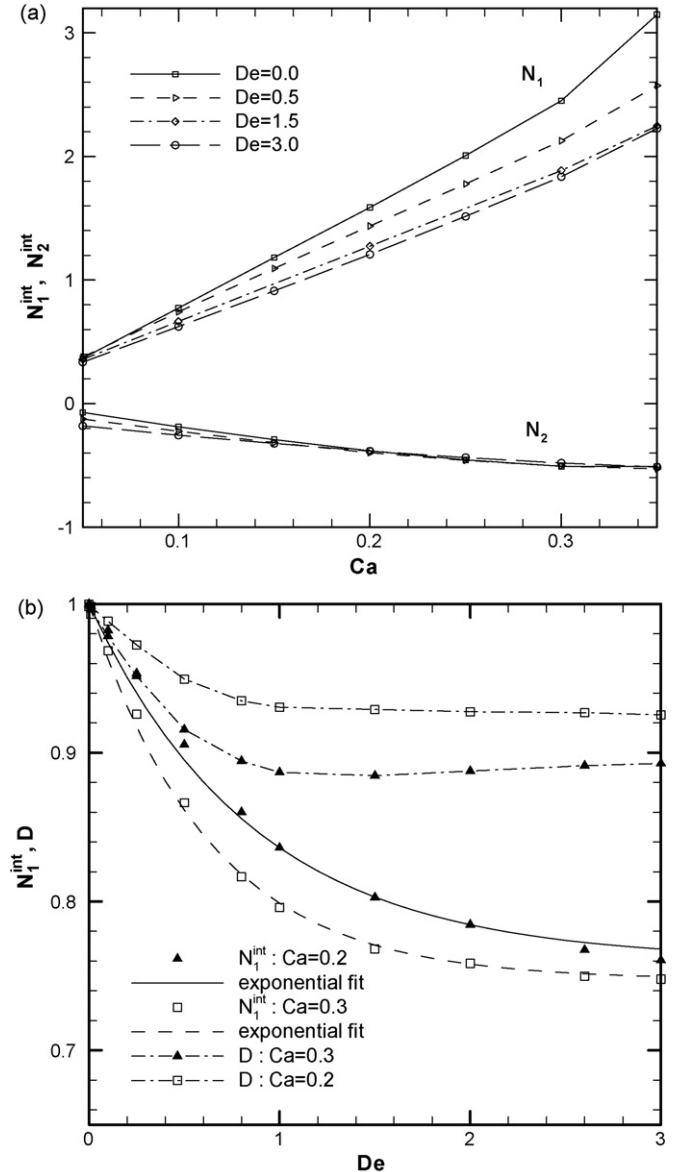


Fig. 4. (a) Variation of interfacial normal stress with Ca . (b) Variation of interfacial normal stress with De .

For comparison, we also plot few analytical results. The small deformation theory of Choi and Schowalter (CS) [8]:

$$\Sigma_{12}^{CS} = \frac{\mu_e^{CS}}{\mu} = \frac{5\lambda + 2}{2(\lambda + 1)} \phi^{\lambda=1} \frac{7}{4} \phi$$

predicts a constant shear viscosity because it does not take into account higher order deformation of the drop. Based on Grmela et al.'s [13] morphological tensor model, Yu et al. [17] described the shear thinning of a viscous emulsion:

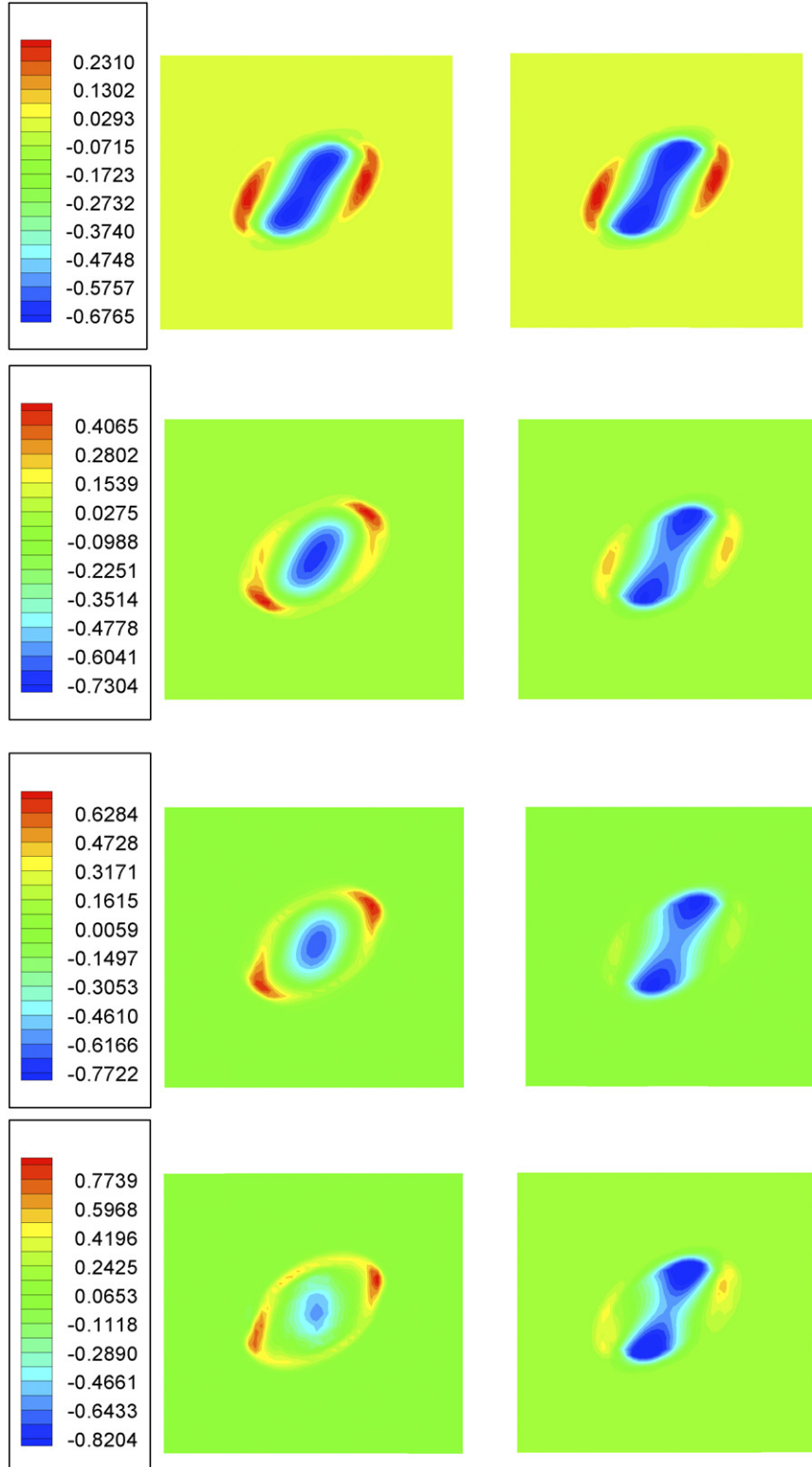


Fig. 5. Plots of viscoelastic stress $T_{xx}^p - T_{yy}^p$ (left column) and $\mu_p(D_{xx} - D_{yy})$ (right column) in the central flow plane for $De = 0.1, 0.5, 1.0$ and 2.0 at $Ca = 0.2$.

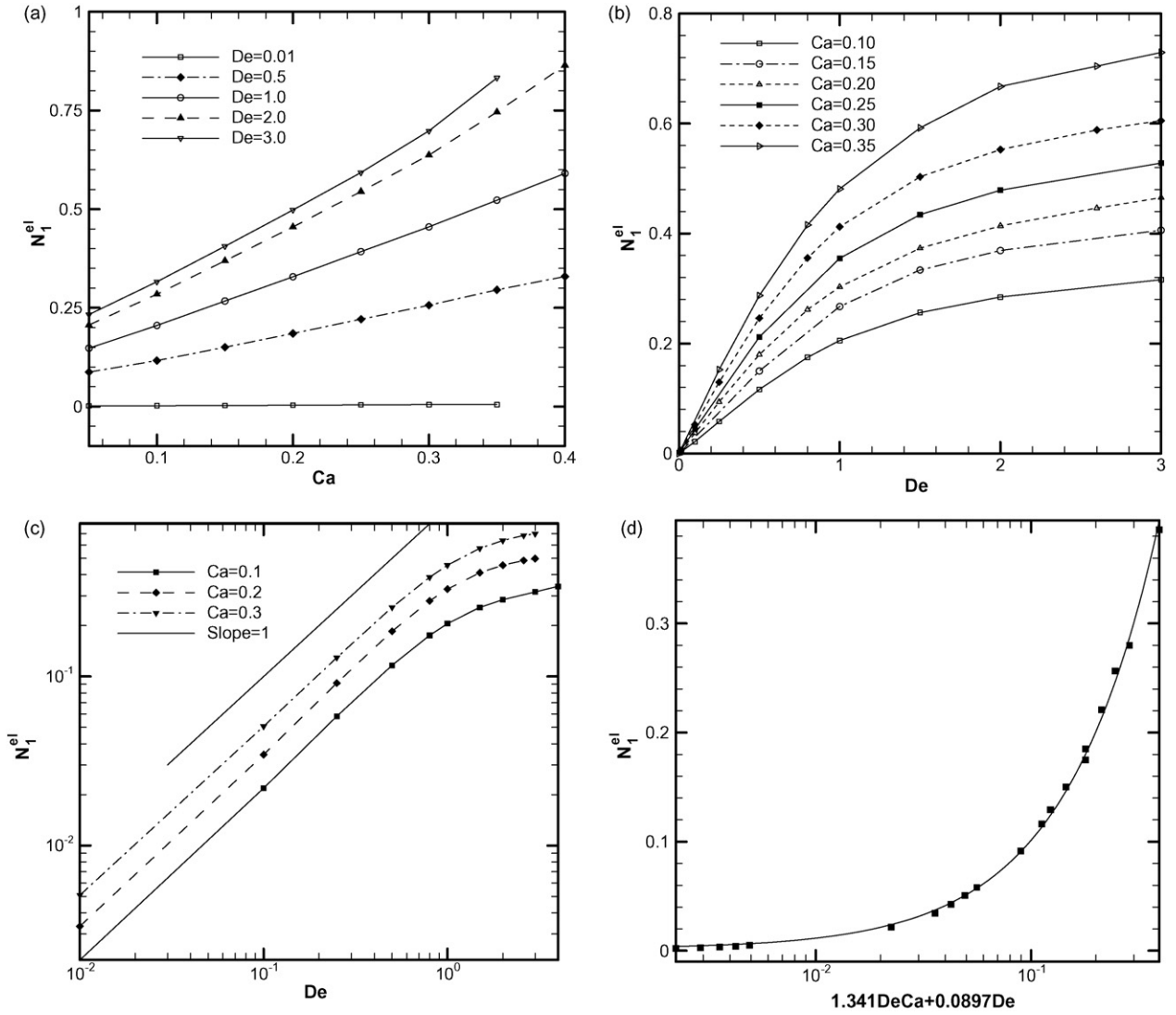


Fig. 6. (a) Viscoelastic first normal stress variation with Ca . (b) Plot of viscoelastic normal stress variation with De . (c) Log–Log plot of viscoelastic normal stress variation with De . (d) Equation describing viscoelastic normal stress contributions.

$$\begin{aligned} \Sigma_{12}^{GBP} &= \frac{\mu_e^{GBP}}{\mu} = \frac{4(2\lambda + 3)}{25} \frac{f_1 f_2^2}{Ca^2 + f_1^2} \phi \\ &= \frac{4(2\lambda + 3)}{25} \frac{f_2^2}{f_1(Z^2 + 1)} \phi \stackrel{\lambda=1}{=} \frac{7}{4} \frac{1}{Z^2 + 1} \phi, \\ f_1 &= \frac{40(\lambda + 1)}{(2\lambda + 3)(19\lambda + 16)} = \frac{Ca \stackrel{\lambda=1}{=} 16}{Z \stackrel{\lambda=1}{=} 35}, \\ f_2 &= \frac{5}{2\lambda + 3} \stackrel{\lambda=1}{=} 1, \\ \text{and } Z &= \frac{(19\lambda + 16)(2\lambda + 3)}{40(\lambda + 1)} Ca \stackrel{\lambda=1}{=} \frac{35}{16} \frac{1}{k}. \end{aligned}$$

The small disparity between our simulation and their analytical prediction is due to the finite amount of inertia ($Re=0.1$) and the finite deformation in our calculation. The change in the shear stress with De is however small. For small Ca , the shear viscosity decreases with increased viscoelasticity, but for larger Ca , it

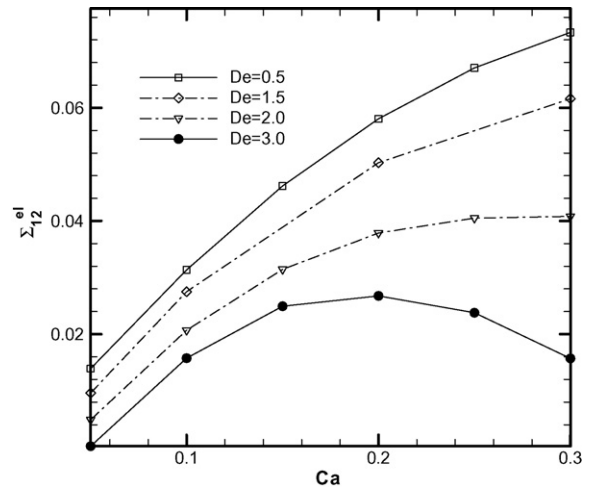


Fig. 7. Variation of viscoelastic shear stress with Ca .

increases. This can be better appreciated from Fig. 3b, where we plot the interfacial contribution to shear viscosity plotted as a function of De for different Ca . From Eqs. (23) and (24), we see that the stresses are governed by the deformation ($n_{1'}^2 - n_{2'}^2$) and the angle θ . Aggarwal and Sarkar [42] showed that

at a fixed Ca , deformation decreases, and the orientation angle increases (towards 45°) with increased De . In Fig. 3b, the shear viscosity contribution (24) shows non-monotonic change with De due to decrease in deformation and a competing increase due to increased θ .

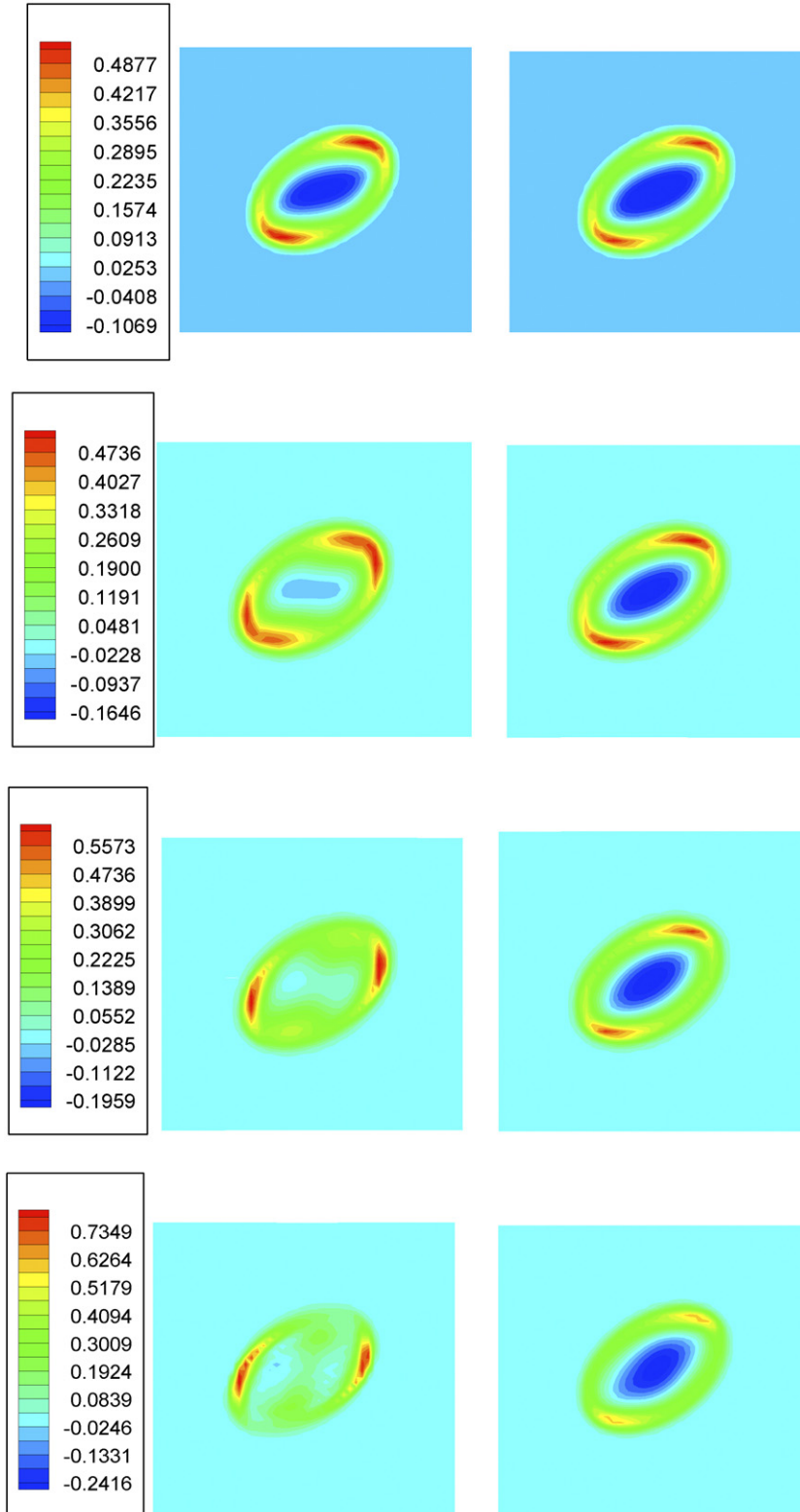


Fig. 8. Plots of viscoelastic stress T_{xy}^p (left column) and $\mu_p D_{xy}$ (right column) in the central flow plane for $De = 0.1, 0.5, 1.0$ and 2.0 at $Ca = 0.2$.

In Fig. 4a, we plot the interfacial contribution to the first and second normal stresses N_1^{int} and N_2^{int} , as functions of Ca . Normal stresses arise due to the anisotropy and orientation of the interface. We see an increase in N_1^{int} with Ca . N_2^{int} also increases in magnitude linearly with Ca . The increase in N_1^{int} with Ca in Fig. 4a can be attributed to an increased drop deformation and its progressive alignment with the flow direction. N_1^{int} goes to zero for $Ca = 0$ at inclination angle $\theta = 45^\circ$. For a fixed Ca value, we see that N_1^{int} decreases with De . This is consistent since drop viscoelasticity inhibits drop deformation as well as orients the drop along the strain-rate ($\theta = 45^\circ$) direction [42,48]. The change in N_2^{int} with De is however very small.

To elucidate the effect of De , we present in Fig. 4b, a plot of N_1^{int} vs. De (N_1^{int} has been scaled with its value for $De = 0$ to accommodate both Ca values). We also present the drop deformation parameter $D = (L - B)/(L + B)$ (due to Taylor [4]) normalized by its viscous value varying with De for the same Ca values from Aggarwal and Sarkar [42]. The plot clearly shows a decrease in N_1^{int} with increasing drop viscoelasticity. It can be explained by noting that the drop viscoelasticity reduces deformation and reduces the orientation (increases θ) of the droplet along the flow direction [Eq. (25)]. The first normal stress shows an exponential decay. It can be explained by noting that the reduction in drop deformation has also been observed to show saturation i.e. there is a maximal contribution of drop elasticity in inhibition of drop deformation [42,55]. For $Ca = 0.3$, although the $D_{\text{st}} \sim De$ curve shows slight non-monotonicity, the $N_1^{\text{int}} \sim De$ monotonically decreases. The effect of the orientation angle dominates the change here.

3.2. Viscoelastic stresses

In contrast to the interfacial contribution, the viscoelastic contribution is an integral of the difference of two terms $-T_{xx} - T_{yy}$ and $\mu_p(D_{xx} - D_{yy})$, over the drop volume [see Eq. (18)]. In Fig. 5, we plot these two fields over the central plane of the drop after the drop has reached a steady state for various De values. For very small value of $De = 0.1$, the two fields are expectedly almost equal, giving rise to a negligible first normal stress. But with increasing De , the difference becomes prominent leading to an enhanced viscoelastic first normal stress N_1^{el} . In Fig. 6a, we plot N_1^{el} in the emulsion, varying with Ca . Non-dimensional N_1^{el} increases linearly with Ca (the slope increases with De). The normal stress contributions vanish for $De \rightarrow 0$. However, we do see a finite N_1^{el} in the limit $Ca \rightarrow 0$, in the limit of an undeformed spherical drop because of the viscoelastic stress in the flow inside. We plot in Fig. 6b, N_1^{el} varying with De for different Ca . Fig. 6c shows the same in log plot to demonstrate $N_1^{\text{el}} \sim De$ for up to $De \sim O(1)$.

In view of the above observations:

$$N_1^{\text{el}} \sim f_1(De) + f_2(De)Ca, \quad N_1^{\text{el}} \sim g_1(Ca)De. \quad (26)$$

We fit the data for N_1^{el} in the range of small Ca and De ($Ca \leq 0.3$ and $De \leq 0.8$) to obtain the equation:

$$N_1^{\text{el}} = 0.0897 De + 1.341 Ca De. \quad (27)$$

Fig. 6d shows this relation. Noting that the deformation is proportional to Ca , the second term indicates the viscoelastic normal stress contribution arising from inside the drop is greater when the drop deforms. This term indicates a departure from the purely volume-fraction based linear mixing rule for estimating the normal stresses due to the viscoelasticity of the components, which is often used in experiments [25,40]. Such a rule does not account for drop deformation. Using this rule, the component contribution, for the normal stress in its dimensional form, due to viscoelasticity of the phases is approximated by

$$N_1^{\text{el(mix)}} = \phi N_1^{\text{d}} + (1 - \phi)N_1^{\text{m}} = \phi \psi_1^{\text{d}} \dot{\gamma}^2 + (1 - \phi) \psi_1^{\text{m}} \dot{\gamma}^2 \quad (28)$$

which translates in our case of a Newtonian matrix as $N_1^{\text{el(mix)}} = \phi \psi_1^{\text{d}} \dot{\gamma}^2$, where ϕ is the volume fraction, ψ_1^{d} is the first normal stress coefficient ($\psi_1 = 2\mu_p \lambda$ for an Oldroyd-B fluid in simple shear), and $\dot{\gamma}$ is the imposed shear rate. Note that in our study we

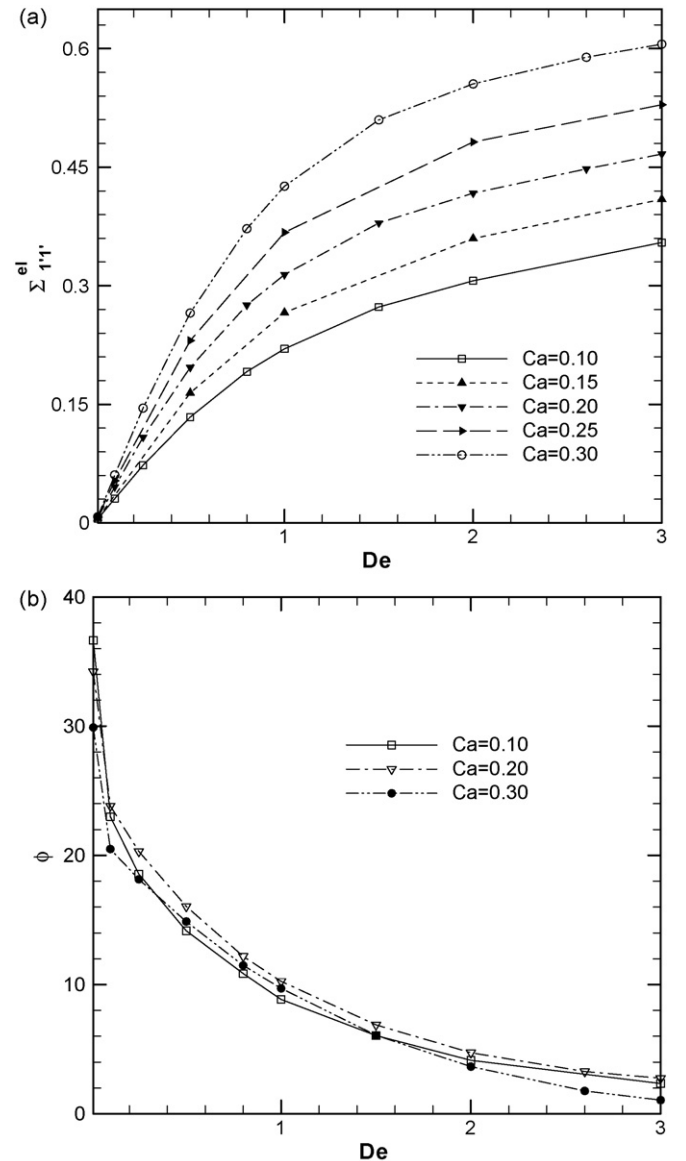


Fig. 9. Primary eigenvalue (a) and eigen-direction (b) of the viscoelastic contribution Σ^{el} .

use only the single drop contribution (i.e. scaled by the volume fraction ϕ); after nondimensionalizing, the expression becomes $N_1^{\text{el(mix)}} = De$ (note $\beta = \mu_p/\mu_d = 0.5$ and $\lambda_\mu = \mu_d/\mu_m = 1.0$). Our simulation enables us to actually compute the component contribution from the stress field. It clearly shows a departure from the mixing rule. If one considers the dimensional contributions, the first term in (27) indicates $N_1^{\text{el}} = 0.0897\phi\mu_m\lambda\dot{\gamma}^2 = 0.179\phi\mu_p\lambda\dot{\gamma}^2 = 0.0897\phi\psi_1^d\dot{\gamma}^2$. The second term in (27) indicates formally a dimensional contribution $N_1^{\text{el}} \propto \lambda|\dot{\gamma}|^3$.

We further note the importance of the $O(CaDe)$ term in the normal stress (27). While analyzing the effect of viscoelasticity on the drop response in steady shear [42], we developed a one dimensional model that represents the dominant physics and explains the observed scaling of deformation D with De and Ca . The surrogate for deformation X in this model was assumed to satisfy:

$$\hat{\mu}\hat{\alpha}^2\dot{X} + \hat{\sigma}\hat{\alpha}X + \hat{N}_1^d\hat{\alpha}^2X = \hat{\mu}\hat{\alpha}^2\dot{\gamma}, \quad (29)$$

where the variables with hat are the model variables for their actual counterparts (i.e. $\hat{\mu}$ is the model viscosity, etc.). The terms in the left represent the viscous, surface tension and first normal stress contribution, and the term in the right is the stretching force due to the imposed shear. We modeled the first normal stress term as $N_1^d = \mu_p\dot{\gamma}^2\lambda\{1 - e^{-t/\lambda}(1 + t/\lambda)\}$, which captured the transient behavior and the steady scaling $X \propto Ca(1 - \beta De Ca)$. Clearly the first normal stress model having a dependence on deformation as in (29), is now justified in view of (27).

In Fig. 7, we plot the shear viscosity contributions due to the drop phase viscoelasticity as a function of Ca . Viscoelasticity of the drop phase does not make significant contributions to the effective shear viscosity of the emulsion, at least in the range of $Ca < Ca_{\text{crit}}$. The observed magnitude of these stresses are negligible in comparison with the interfacial shear stress contributions. Note that due to the definition that we adopted for the viscoelastic component contribution (18), the shear stress part

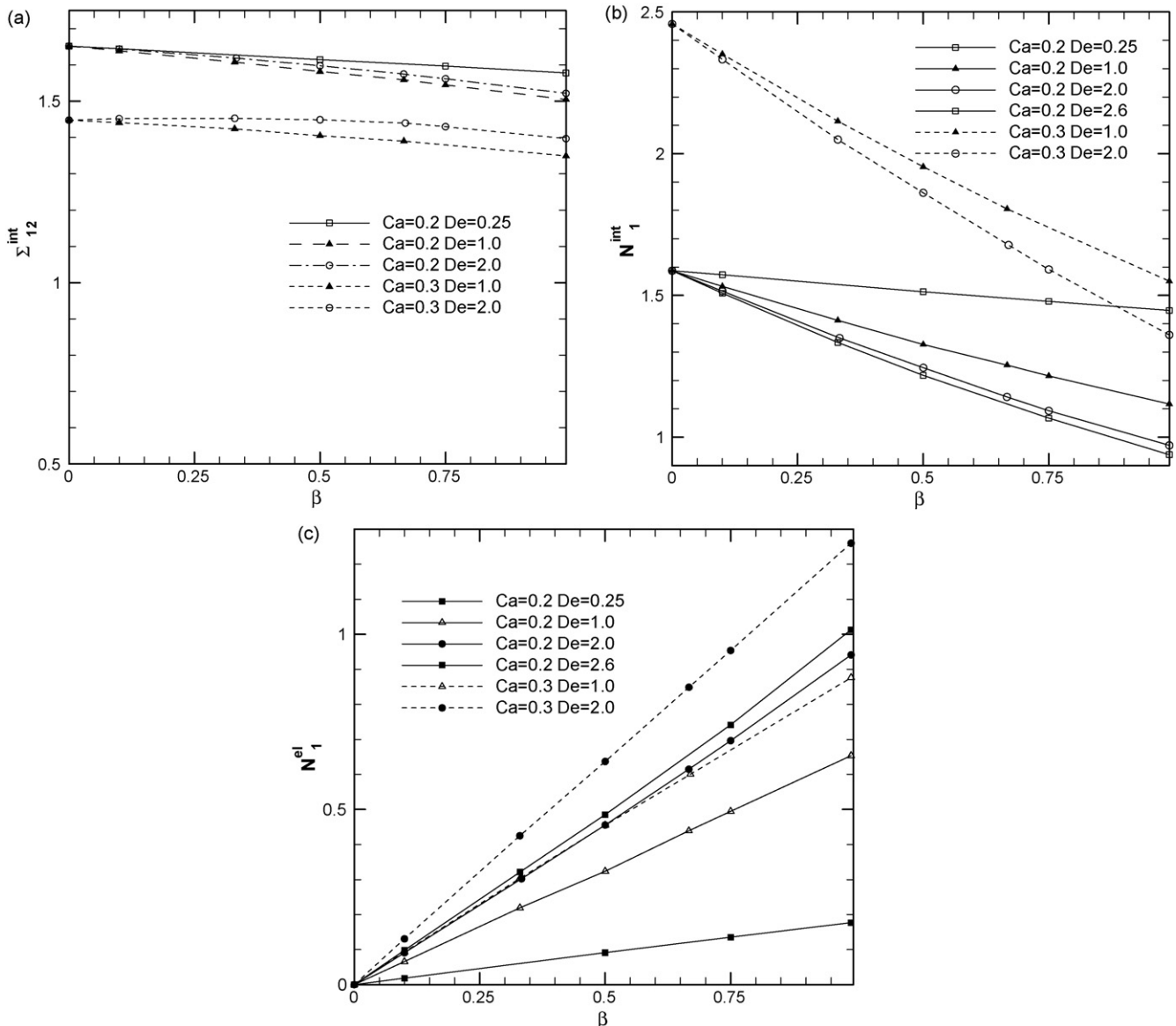


Fig. 10. (a) Variation in interfacial shear stress with β . (b) Variation in interfacial normal stress vs. β . (c) Variation in viscoelastic normal stress with β .

is an integral of a difference between the actual polymeric shear stress T_{xy}^p and the instantaneous viscous stress $\mu_p D_{xy}$ computed using the local strain rate. In Fig. 8, we plot them in the central flow plane of the drop for several different De and $Ca = 0.2$. Note that both T_{xy}^p and $\mu_p D_{xy}$ for each De are on the same color scale. It is clear that the shear contributions are negligible not due to a point-wise cancellation. They are different yet the volume integral $\int_{V_0} (T_{xy} - \mu_p D_{xy}) dV$ is negligible.

We further investigate the viscoelastic stress contributions by looking at the eigenvalues and the eigen-directions of the Σ_d^{el} tensor. In Fig. 9a, we plot the primary eigenvalue Σ_{11}^{el} and in Fig. 9b we plot the orientation of the primary eigen-direction φ with reference to the flow direction as a function of De for different Ca . We note that the other two eigenvalues (not shown here) are negligible indicating a strong anisotropy in this tensor. Note the strong similarity in trend between Σ_{11}^{el} and N_1^{el} shown in

Fig. 6b even though the later consists of Cartesian components. Moreover, the dominant eigenvalue is oriented towards the flow direction (hence $N_1^{el} > 0$). With increasing De the orientation with the flow is further enhanced (within 3° for $De = 3$), indicating that the principal direction is almost in the flow direction. Therefore, the rheological contribution of drop viscoelasticity is a tensile stress of magnitude Σ_{11}^{el} (resisting drop deformation) with negligible contribution to effective emulsion shear viscosity.

3.3. Variation of parameter β

We also investigate the effect of varying parameter β ($\beta = \mu_{pd}/\mu_d$) on the steady shear rheology, while keeping the viscosity ratio λ_μ constant (i.e. $\lambda_\mu = 1$ for our study). For $\beta = 1.0$ we get an Upper Convected Maxwell constitutive equation. An

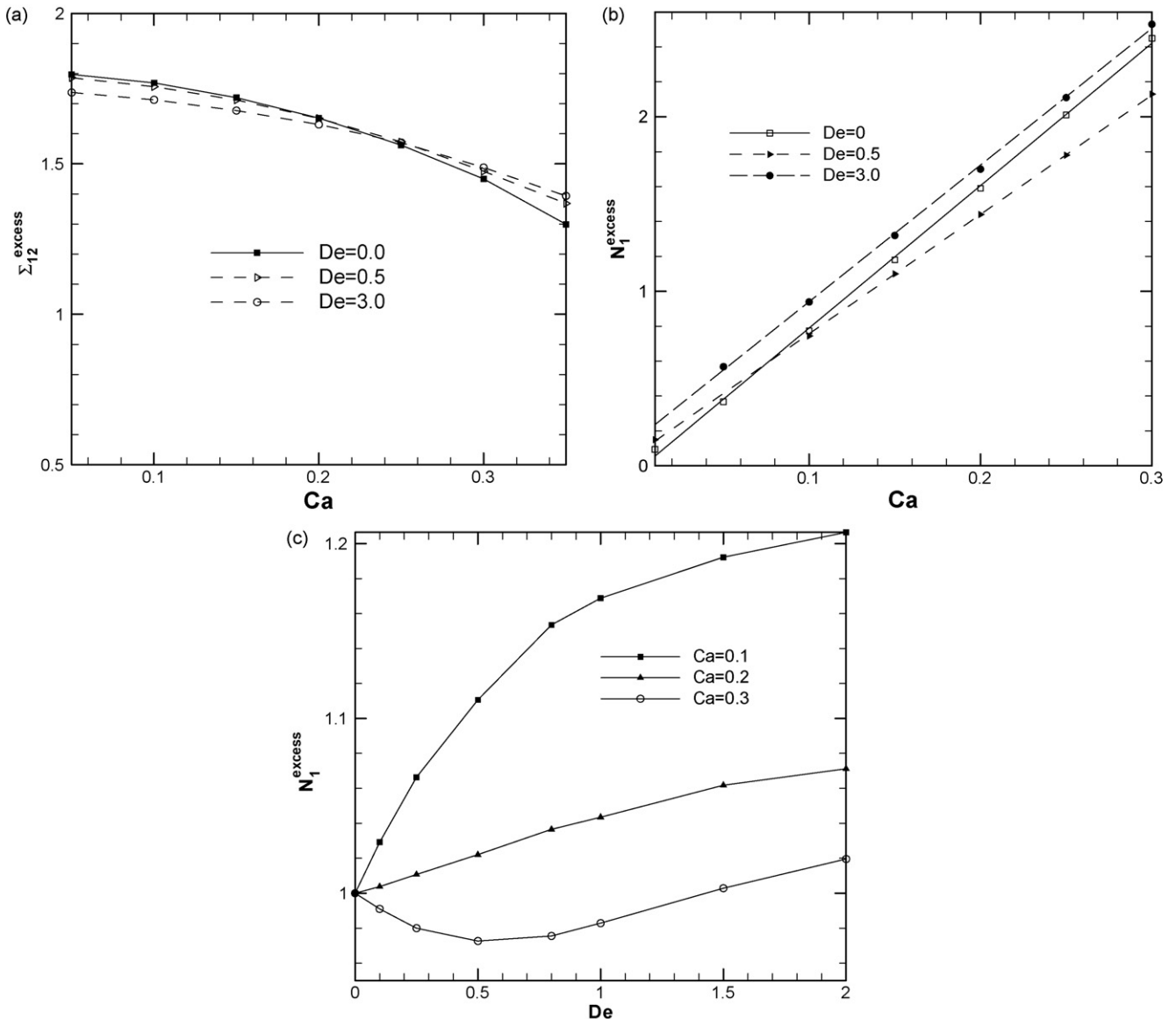


Fig. 11. (a) Variation of excess shear stresses with Ca . (b) Variation of excess normal stresses with Ca . (c) Variation of excess normal stresses with De (normalized with its $De = 0$ value).

increase in β , for constant De , is equivalent to increasing the viscoelastic contributions in the drop phase.

In Fig. 10a, we plot the variation of the interfacial shear stress with β . Σ_{12}^{int} decreases slightly with β because of the observed linear decrease in drop deformation with β in Aggarwal and Sarkar [42], the effect being more prominent for high values of β . In Fig. 10b, we plot variation of the interfacial contribution to the first normal stress difference N_1^{int} with parameter β for different sets of Ca and De . The stress contribution decreases linearly, indicative of the linear decrease in steady drop deformation D with β previously noted by Aggarwal and Sarkar [42]. In Fig. 10c, we plot the viscoelastic contributions to the first normal stress difference N_1^{el} with varying β . N_1^{el} increases linearly with β over the entire range of the parameter values as expected.

Finally, in Fig. 11 we plot the total excess shear stress contributions $\Sigma_{12}^{\text{excess}}$ and N_1^{excess} due to the dispersed viscoelastic phase in the emulsion. The effect of drop phase viscoelasticity on shear viscosity is modest (Fig. 11a). As expected, N_1^{excess} is linear with Ca (Fig. 11b). The plots for $De = 0$ and $De = 0.5$ intersect, indicating the competition between increase in the elastic component N_1^{el} with De and the decrease in the interfacial component N_1^{int} (with De). It is further elucidated in Fig. 11c, where the excess stress is plotted as a function of De for various Ca . The stress is normalized by its Newtonian ($De = 0$) value. The curves for $Ca = 0.1$ and $Ca = 0.2$ shows an increase in excess normal stress with De , but the $Ca = 0.3$ plot shows a non-monotonic trend.

4. Summary

We have used simulation of single viscoelastic drop dynamics to investigate the rheology of a dilute emulsion consisting of such drops suspended in a Newtonian matrix. The simulation is performed using a front-tracking method. The effective stress in a viscoelastic emulsion consists of three components—due to the interface, due to dispersed phase viscoelasticity and due to the difference in viscosities of the two phases. We restrict ourselves to a viscosity matched system. The interfacial contribution is affected by the viscoelasticity and vice versa. The interfacial contribution is purely geometric, and therefore can be explained by the drop response. Shear thinning of a viscous emulsion is modified by the drop phase viscoelasticity. The shear viscosity is reduced from its Newtonian value by viscoelasticity for low Ca and enhanced for high Ca due to the competing effects of decreased deformation and decreased drop alignment with the flow. For the case of purely viscous systems, N_1^{int} and N_2^{int} are found to change linearly with the Capillary number. The drop response decreases the first normal stress with increasing viscoelasticity.

The component contribution due to drop phase viscoelasticity is computed directly from the simulated stress field. While not changing the shear viscosity substantially, it contributes to the first normal stress difference N_1 in the emulsion. The viscoelastic contribution manifests as an anisotropic tensile stress in the principal co-ordinate system, that increases linearly in magnitude with De [for $De \sim O(1)$]. The orientation of this tensile stress is always less than 45° (measured from the flow direc-

tion) and further decreases with increasing viscoelasticity. We find that this component contribution N_1^{el} has two terms αDe and $\alpha De Ca$. The second term indicates a departure from the linear mixing rule commonly adopted while analyzing experiments involving viscoelastic phases. Variations in the polymeric contributions to the total drop viscosity β , causes a linear change in N_1^{el} with insignificant change in Σ_{12}^{el} .

The overall excess first normal stress shows an increase with Deborah number for low Capillary numbers. However for high Capillary numbers, it shows a non-monotonic behavior due to the competition between the viscoelastic part and interfacial parts, in that it first decreases due to decreased drop deformation, and finally increases due to increasing viscoelastic component stress.

Acknowledgement

Partial support for this work is obtained from National Science Foundation NSF-CBET 0625599.

References

- [1] C.L. Tucker, P. Moldenaers, Microstructural evolution in polymer blends, *Annu. Rev. Fluid Mech.* 34 (2002) 177–210.
- [2] A. Einstein, Eine neue bestimmung der Molekul-dimension, *Ann. Phys.* 19 (1906) 289–306.
- [3] A. Einstein, Berichtigung Zu meiner Arbeit: Eine neue bestimmung der Molekul-dimension, *Ann. Phys.* 34 (1911) 591–592.
- [4] G.I. Taylor, The viscosity of a fluid containing small drops of another fluid, *Proc. R. Soc. Lond. A* 138 (1932) 41–48.
- [5] J.G. Oldroyd, The effect of interfacial stabilizing films on the elastic and viscous properties of emulsions, *Proc. R. Soc. Lond. Ser. A: Math. Phys. Sci.* 232 (1955) 567–577.
- [6] J.G. Oldroyd, The elastic and viscous properties of emulsions and suspensions, *Proc. R. Soc. Lond. Ser. A: Math. Phys. Sci.* 218 (1953) 122–132.
- [7] W.R. Schowalter, C.E. Chaffey, H. Brenner, Rheological behavior of a dilute emulsion, *J. Colloid Interface Sci.* 26 (1968), 152–&.
- [8] S.J. Choi, W.R. Schowalter, Rheological properties of non-dilute suspensions of deformable particles, *Phys. Fluids* 18 (1975) 420–427.
- [9] G.K. Batchelor, Stress system in a suspension of force-free particles, *J. Fluid Mech.* 41 (1970) 545.
- [10] J. Mellema, M.W.M. Willemsse, Effective viscosity of dispersions approached by a statistical continuum method, *Physica A* 122 (1983) 286–312.
- [11] A. Onuki, Viscosity enhancement by domains in phase-separating fluids near the critical-point—proposal of critical rheology, *Phys. Rev. A* 35 (1987) 5149–5155.
- [12] W. Yu, M. Bousmina, Ellipsoidal model for droplet deformation in emulsions, *J. Rheol.* 47 (2003) 1011–1039.
- [13] M. Grmela, M. Bousmina, J.F. Paliarne, On the rheology of immiscible blends, *Rheol. Acta* 40 (2001) 560–569.
- [14] E.D. Wetzel, C.L. Tucker, Droplet deformation in dispersions with unequal viscosities and zero interfacial tension, *J. Fluid Mech.* 426 (2001) 199–228.
- [15] P.L. Maffettone, M. Minale, Equation of change for ellipsoidal drops in viscous flow, *J. Non-Newton. Fluid Mech.* 78 (1998) 227–241.
- [16] N.E. Jackson, C.L. Tucker, A model for large deformation of an ellipsoidal droplet with interfacial tension, *J. Rheol.* 47 (2003) 659–682.
- [17] W. Yu, M. Bousmina, M. Grmela, J.F. Paliarne, C.X. Zhou, Quantitative relationship between rheology and morphology in emulsions, *J. Rheol.* 46 (2002) 1381–1399.
- [18] W. Yu, M. Bousmina, M. Grmela, C.X. Zhou, Modeling of oscillatory shear flow of emulsions under small and large deformation fields, *J. Rheol.* 46 (2002) 1401–1418.

- [19] T. Jansseune, J. Mewis, P. Moldenaers, M. Minale, P.L. Maffettone, Rheology and rheological morphology determination in immiscible two-phase polymer model blends, *J. Non-Newton. Fluid Mech.* 93 (2000) 153–165.
- [20] T. Jansseune, I. Vinckier, P. Moldenaers, J. Mewis, Transient stresses in immiscible model polymer blends during start-up flows, *J. Non-Newton. Fluid Mech.* 99 (2001) 167–181.
- [21] M. Doi, T. Ohta, Dynamics and rheology of complex interfaces. 1, *J. Chem. Phys.* 95 (1991) 1242–1248.
- [22] Y. Takahashi, N. Kurashima, I. Noda, M. Doi, Experimental tests of the scaling relation for textured materials in mixtures of 2 immiscible fluids, *J. Rheol.* 38 (1994) 699–712.
- [23] I. Vinckier, P. Moldenaers, J. Mewis, Transient rheological response and morphology evolution of immiscible polymer blends, *J. Rheol.* 41 (1997) 705–718.
- [24] I. Vinckier, P. Moldenaers, J. Mewis, Relationship between rheology and morphology of model blends in steady shear flow, *J. Rheol.* 40 (1996) 613–631.
- [25] Y. Takahashi, S. Kitade, N. Kurashima, I. Noda, Viscoelastic properties of immiscible polymer blends under steady and transient shear flows, *Polym. J.* 26 (1994) 1206–1212.
- [26] M. Bousmina, M. Aouina, B. Chaudhry, R. Guenette, R.E.S. Bretas, Rheology of polymer blends: non-linear model for viscoelastic emulsions undergoing high deformation flows, *Rheol. Acta* 40 (2001) 538–551.
- [27] M. Grmela, A. Aitkadi, Comments on the Doi–Ohta theory of blends, *J. Non-Newton. Fluid Mech.* 55 (1994) 191–195.
- [28] M. Grmela, A. Ait-Kadi, Rheology of inhomogeneous immiscible blends, *J. Non-Newton. Fluid Mech.* 77 (1998) 191–199.
- [29] N.J. Wagner, H.C. Ottinger, B.J. Edwards, Generalized Doi–Ohta model for multiphase flow developed via GENERIC, *AIChE J.* 45 (1999) 1169–1181.
- [30] H.M. Lee, O.O. Park, Rheology and dynamics of immiscible polymer blends, *J. Rheol.* 38 (1994) 1405–1425.
- [31] A.S. Almusallam, R.G. Larson, M.J. Solomon, Comprehensive constitutive model for immiscible blends of Newtonian polymers, *J. Rheol.* 48 (2004) 319–348.
- [32] G.W.M. Peters, S. Hansen, H.E.H. Meijer, Constitutive modeling of dispersive mixtures, *J. Rheol.* 45 (2001) 659–689.
- [33] J.F. Palierne, Linear rheology of viscoelastic emulsions with interfacial tension, *Rheol. Acta* 29 (1990) 204–214.
- [34] J.F. Palierne, Correction, *Rheol. Acta* 30 (1991) 497.
- [35] D. Graebbling, R. Muller, J.F. Palierne, Linear viscoelastic behavior of some incompatible polymer blends in the melt—interpretation of data with a model of emulsion of viscoelastic liquids, *Macromolecules* 26 (1993) 320–329.
- [36] C. Lacroix, M. Bousmina, P.J. Carreau, B.D. Favis, A. Michel, Properties of PETG/EVA blends. I. Viscoelastic, morphological and interfacial properties, *Polymer* 37 (1996) 2939–2947.
- [37] M. Bousmina, Rheology of polymer blends: linear model for viscoelastic emulsions, *Rheol. Acta* 38 (1999) 73–83.
- [38] E.H. Kerner, The elastic and thermo-elastic properties of composite media, *Proc. Phys. Soc. Lond. Sect. B* 69 (1956) 808–813.
- [39] W. Yu, M. Bousmina, C.X. Zhou, C.L. Tucker, Theory for drop deformation in viscoelastic systems, *J. Rheol.* 48 (2004) 417–438.
- [40] V. Cristini, C.W. Macosko, T. Jansseune, A note on transient stress calculation via numerical simulations, *J. Non-Newton. Fluid Mech.* 105 (2002) 177–187.
- [41] G. Tryggvason, B. Bunner, A. Esmaeeli, D. Juric, N. Al-Rawahi, W. Tauber, J. Han, S. Nas, Y.J. Jan, A front-tracking method for the computations of multiphase flow, *J. Comput. Phys.* 169 (2001) 708–759.
- [42] N. Aggarwal, K. Sarkar, Deformation and breakup of a viscoelastic drop in a Newtonian matrix under steady shear, *J. Fluid Mech.* 584 (2007) 1–21.
- [43] K. Sarkar, W.R. Schowalter, Deformation of a two-dimensional viscoelastic drop at non-zero Reynolds number in time-periodic extensional flows, *J. Non-Newton. Fluid Mech.* 95 (2000) 315–342.
- [44] D.B. Khismatullin, Y. Renardy, M. Renardy, Development and implementation of VOF-PROST for 3D viscoelastic liquid–liquid simulations, *J. Non-Newton. Fluid Mech.* 140 (2006) 120–131.
- [45] P.L. Maffettone, F. Greco, Ellipsoidal drop model for single drop dynamics with non-Newtonian fluids, *J. Rheol.* 48 (2004) 83–100.
- [46] S. Ramaswamy, L.G. Leal, The deformation of a Newtonian drop in the uniaxial extensional flow of a viscoelastic liquid, *J. Non-Newton. Fluid Mech.* 88 (1999) 149–172.
- [47] S. Ramaswamy, L.G. Leal, The deformation of a viscoelastic drop subjected to steady uniaxial extensional flow of a Newtonian fluid, *J. Non-Newton. Fluid Mech.* 85 (1999) 127–163.
- [48] P.T. Yue, J.J. Feng, C. Liu, J. Shen, Viscoelastic effects on drop deformation in steady shear, *J. Fluid Mech.* 540 (2005) 427–437.
- [49] X.Y. Li, K. Sarkar, Drop dynamics in an oscillating extensional flow at finite Reynolds numbers, *Phys. Fluids* 17 (2005), 027103.
- [50] X.Y. Li, K. Sarkar, Numerical investigation of the rheology of a dilute emulsion of drops in an oscillating extensional flow, *J. Non-Newton. Fluid Mech.* 128 (2005) 71–82.
- [51] X.Y. Li, K. Sarkar, Negative normal stress elasticity of emulsions of viscous drops at finite inertia, *Phys. Rev. Lett.* 95 (2005), 256001.
- [52] X.Y. Li, K. Sarkar, Effects of inertia on the rheology of a dilute emulsion of drops in shear, *J. Rheol.* 49 (2005) 1377–1394.
- [53] X.F. Li, R. Charles, C. Pozrikidis, Simple shear flow of suspensions of liquid drops, *J. Fluid Mech.* 320 (1996) 395–416.
- [54] M. Loewenberg, E.J. Hinch, Numerical simulation of a concentrated emulsion in shear flow, *J. Fluid Mech.* 321 (1996) 395–419.
- [55] F. Mighri, P.J. Carreau, A. Ajji, Influence of elastic properties on drop deformation and breakup in shear flow, *J. Rheol.* 42 (1998) 1477–1490.